

## SYNTHESIS, GROWTH, CRYSTAL STRUCTURE AND CHARACTERIZATION OF AN ORGANIC SALT SINGLE CRYSTAL: DIIMIDAZOLIUM DIPCATE MONOHYDRATE

### ABSTRACT

The organic salt of Diimidazolium dpicrate monohydrate (DIDPMH) has been synthesized and single crystals grown by slow solvent evaporation solution growth technique at room temperature using dry acetonitrile as the solvent. The  $^1\text{H}$  and  $^{13}\text{C}$  NMR spectra were recorded to confirm the presence of different proton environments and different kinds of carbon atoms respectively. The molecular structure of the title crystal was established by single crystal X-ray diffraction technique and it belongs to monoclinic crystal system with the space group  $P2_1/m$  and the unit cell parameters are  $a=6.8527(3)$  Å,  $b=23.4396(2)$  Å,  $c=8.1335(6)$  Å. The functional groups present in the crystal were confirmed by FT-IR analysis. The optical transmittance window and the lower cut-off wavelength of the DIDPMH crystal have been identified by UV-Vis-NIR transmittance study. A fluorescence emission study shows that the title crystal has green-orange fluorescence emission. The second harmonic generation (SHG) was confirmed by modified Kurtz-Perry powder method and it is found to be 0.2 times that of potassium dihydrogen phosphate (KDP) crystal. The thermal stability of the title crystal was investigated by TG/DTA analyses and differential scanning calorimetry. The surface morphology of the grown DIDPMH crystal was studied by scanning electron microscopy (SEM).

**Keywords** Organic materials; Nonlinear optical; X-ray diffraction; Solution growth; Single crystal.

### 1. INTRODUCTION

The non-centrosymmetric arrangement of molecules in the crystal lattice with large second order nonlinearities are in great demand for their nonlinear optical applications. The organic materials are expected to have relatively strong nonlinear optical (NLO) properties due to the presence of delocalized  $\pi$ -electron systems linking donor and acceptor groups which enhance the necessary asymmetric polarizability. This expectation explains extensive search for better NLO materials among organic crystals. Such materials have much greater design flexibility than inorganic compounds, which allows them to be tailored for designing and obtaining novel processible nonlinear optical (NLO) materials and their structures can be modified to get the desired NLO properties which leads to fast optical response [1-4]. Recently, the five membered aromatic heterocyclic imidazole derivatives have attracted to a considerable extent, because the imidazole ring system is present in important biological molecules, such as histidine and the related hormone histamine. Many drugs contain an imidazole ring, such as antifungal drugs, nitroimidazole, azomycin and metronidazole. So imidazole has become an important part of many pharmaceuticals [5-7]. The imidazoles have also found application as a chromophore with readily tunable absorption wavelength, fluorophoric properties and synthetic building blocks in supramolecular chemistry [8]. It was already reported that the imidazole ring bonds react with picric acid molecule and forms a salt of imidazolium picrate in acetone, which crystallizes in the orthorhombic system with space group  $pbca$  and the structural, optical, mechanical and vibrational properties of the salt were also investigated [9-11]. Moreno-Fuquen et al have reported the crystal structure of Imidazole-Imidazolium picrate monohydrate compound using imdazole and picric acid as the starting materials in the ratio of 2:1 in dry acetonitrile as the solvent. It crystallizes in the orthorhombic crystal structure with non-centrosymmetric space group  $P2_12_12_1$  [12]. Sincere attempts were made to synthesize the same compound and grow the crystals of it employing the procedure available in the literature to investigate other properties of the material. But surprisingly, we obtained a new crystal which crystallizes in the monoclinic crystal system with centrosymmetric space group  $P2_1/m$ . In this paper, we report the synthesis, crystal structure, spectral, optical and thermal characterizations of the diimidazolium dpicrate monohydrate salt crystal.

### 2. EXPERIMENTAL PROCEDURE

#### 2.1 Material synthesis and growth of DIDPMH single crystals

Analar grade imidazole and picric acid were obtained from loba chemie and used as such without additional purification. The title compound was synthesized by dissolving imidazole and picric acid in dry acetonitrile separately in the molar ratio of 2:1 and henceforth

mixed together. The resulting solution was stirred well for six hours. Suspended impurities were removed by using whatmann 41 grade filter paper. The clear filtrate so obtained was kept aside unperturbed in a dust free room for the growth of single crystals. The reaction involved in the synthesis of DIDPMH complex is shown in the Figure 1. Well defined, yellow colored single crystals were collected after a week. The photograph of as-grown crystal of DIDPMH is shown in Figure 2.

## 2.2 Characterization techniques

The grown single crystals of DIDPMH were subjected to various characterization techniques like  $^1\text{H}$  and  $^{13}\text{C}$  NMR spectral analyses, Fourier transform infrared (FT IR), UV-Vis-NIR transmittance studies, TG/DTA analyses, scanning electron microscopy, differential scanning calorimetry (DSC), fluorescence emission study and Kurtz-Perry powder SHG test. The structure of the grown DIDPMH has been examined using a 'ENRAF (BRUKER) NONIUS CAD4' single crystal X-ray diffractometer with graphite monochromated  $\text{MoK}\alpha$  radiation ( $\lambda=0.71073 \text{ \AA}$ ). A good optical quality colorless single crystal of dimension  $0.30 \times 0.20 \times 0.01 \text{ mm}$  was selected for diffraction analysis. A total of 19489 reflections (2188 Unique,  $R(\text{int})=0.0830$ ) were collected by using an  $\omega/2\theta$  scan mode at  $293(2) \text{ K}$  in the range of  $2.70^\circ < \theta < 25.00^\circ$  with the index range  $-8 \leq h \leq 8$ ,  $-27 \leq k \leq 27$ ,  $-9 \leq l \leq 9$ . The structures were solved by direct methods and refined by the full-matrix least-squares method on  $F^2$  using the SHELXS-97 [13] crystallographic software package. All non-hydrogen atoms were refined using anisotropic displacement parameters. All hydrogen atoms were placed in the riding mode and refined isotropically. The  $^1\text{H}$  and  $^{13}\text{C}$  NMR spectra were recorded employing a 'BRUKER AVANCE III 500 MHz (AV 500) spectrometer with TMS as the internal reference standard and DMSO as the solvent. The optical transmission spectrum of DIDPMH crystals were recorded in the region 200-1100 nm employing a Shimadzu UV-1061 UV-Vis spectrophotometer in DMSO solution. The FT-IR spectrum of the DIDPMH crystal was recorded employing a SHIMADZU model IR Affinity-1 spectrometer in the range  $4000\text{-}400 \text{ cm}^{-1}$  following the KBr pellet technique. The fluorescence emission spectrum of DIDPMH crystal was recorded using HORIBA JASCO V-670 Fluorolog 3 spectrofluorometer. The TGA (thermogravimetric analysis) and DTA (differential thermal analysis) traces of the sample were taken using a STA 409 PL LUX thermal analyzer with a heating rate of  $10 \text{ K/min}$  in nitrogen atmosphere in the temperature range of  $26^\circ$  to  $500^\circ$ . The differential scanning calorimetric (DSC) analysis was carried out using STA 409 PL LUX DSC between  $26$  and  $600^\circ\text{C}$  in the nitrogen atmosphere at a heating rate of  $10\text{K/min}$ . The SHG property of DIDPMH was tested by employing the modified Kurtz and Perry powder SHG test using a Q-switched Nd:YAG laser ( $1064 \text{ nm}$ ) and KDP was used as the reference material. The surface morphology of the DIDPMH crystal was studied using a INCA penta FETX3 scanning electron microscope.

## 3. RESULTS AND DISCUSSION

### 3.1 $^1\text{H}$ and $^{13}\text{C}$ Nuclear magnetic resonance spectroscopic studies

The  $^1\text{H}$  NMR spectrum depicted in Figure 3 exhibits of five proton signals which indicate the presence of five different proton environments in the title crystal. The broad hump appearing at  $\delta 14.19 \text{ ppm}$  is assigned to the highly deshielded  $^+\text{N-H}$  protons. The intense singlet signal appearing at  $\delta 9.09 \text{ ppm}$  has been assigned to C5 aromatic proton of imidazolium moiety. The singlet peak at  $\delta 8.59 \text{ ppm}$  is assigned to the C3 and C5 aromatic protons of the same kind in picrate moiety. The C2 and C3 aromatic protons of imidazolium moiety appear as a doublet in the aromatic region of the spectrum at  $\delta 7.69 \text{ ppm}$ . The splitting of the signal into doublet is due to coupling of C2 and C3 protons with each other. The hump at  $\delta 3.50 \text{ ppm}$  is assigned to the protons of water of crystallization.

The  $^{13}\text{C}$  NMR spectrum of the title crystal is depicted in Figure 4. The appearance of six distinct peaks in the spectrum establishes the molecular structure of the DIDPMH complex salt. The weak signal appearing at  $\delta 161.30 \text{ ppm}$  has been assigned to the ipso carbon (C1) in the picrate moiety. The signal at  $\delta 142.31 \text{ ppm}$  is attributed to the C2 and C6 carbon atoms of the same kind in picrate moiety. The signal due to C3 and C5 carbon atoms of the same kind in picrate moiety appear as an intense signal at  $\delta 125.67 \text{ ppm}$ . The signal at  $\delta 124.72 \text{ ppm}$  owes to the C4 carbon atom of the same moiety in the complex. The signal at  $\delta 134.84 \text{ ppm}$  owes to the C2 and C3 carbon atoms of the same kind in the imidazolium moiety. The signal due to C5 carbon atom in the imidazolium moiety appears at  $\delta 119.76 \text{ ppm}$ .

### 3.2 Fourier transform infrared spectroscopy

The FT-IR spectrum of DIDPMH was recorded in the range  $4000\text{-}400 \text{ cm}^{-1}$  (Figure 5). It is evident from the spectrum that the band at

3339  $\text{cm}^{-1}$  is assigned to the OH asymmetric stretching vibration. The band observed at 3147  $\text{cm}^{-1}$  is assigned to  $\text{N}^+$ -H stretching vibration. The bands at 3083 and 2920  $\text{cm}^{-1}$  due to aromatic C-H asymmetric and symmetric stretching vibrations respectively. The C-H asymmetric stretching vibration of the imidazolium ring overlaps with the aromatic C-H asymmetric stretching vibration and the corresponding C-H symmetric stretching vibration are observed at 2998  $\text{cm}^{-1}$ . The bands at 1607 and 1486  $\text{cm}^{-1}$  are assigned to the aromatic C=C stretching vibrations. The bands at 1550 and 1323  $\text{cm}^{-1}$  due to  $\text{NO}_2$  asymmetric and symmetric stretching vibrations respectively. A band at 1280  $\text{cm}^{-1}$  corresponds to the O-H inplane bending vibration. A band at 1166  $\text{cm}^{-1}$  is assigned to the C-O stretching vibration. The band observed at 1089  $\text{cm}^{-1}$  is assigned to C-H inplane bending vibration of imidazolium ring. The C-N stretching vibration of nitro group is observed at 911  $\text{cm}^{-1}$ . The respective assignments are given in Table 1.

### 3.3 Single crystal X-ray diffraction analysis

The crystal data and details of the data collection and the structure refinement are given in Table 2. The DIDPMH crystal belongs to the monoclinic crystal system with space group  $\text{P2}_1/\text{m}$  and its unit cell dimensions are determined as  $a=6.8527(3)$  Å,  $b=23.4396(2)$  Å,  $c=8.1335(6)$  Å,  $V=1212.91(10)$  Å<sup>3</sup>. Selected bond lengths and bond angles of the complex are listed in Table 3 and Table 4 respectively. The ORTEP plot of DIDPMH is shown in Figure 6 and the molecular packing arrangement is viewed down in the c axis and b axis as shown respectively in Figure 7 and Figure 8. The intermolecular hydrogen bonding interaction between the molecules in three dimensional network arrangement is shown in Figure 9. The asymmetric part of DIDPMH contains two cationic imidazolium moiety, two picrate anion and one water molecule. The five intermolecular hydrogen bonds are observed in DIDPMH crystal and the corresponding data for the H-bonds are listed in Table 5. The symmetrical intermolecular hydrogen bonds were found between  $\text{N}(4)\text{-H}(4\text{A})\cdots\text{O}(6)$  [ $-x+2,-y,-z+1$ ],  $\text{N}(4)\text{-H}(4\text{A})\cdots\text{O}(1)$  [ $x,y,z-1$ ],  $\text{N}(5)\text{-H}(5)\cdots\text{O}(8)$  [ $x,-y+1/2,z$ ],  $\text{N}(6)\text{-H}(9')\cdots\text{O}(7)$  [ $x+1,y,z$ ] with a donor-acceptor distances of 3.066(6)Å, 3.185(6)Å, 2.701(7)Å, 3.03(3)Å respectively. The  $\text{O}(8)\text{-H}(8\text{A})\cdots\text{O}(7)$  [ $x,-y+1/2,z-1$ ] hydrogen bond  $d(\text{H}\cdots\text{A})$  distance are 1.97(2)Å. The intermolecular and intramolecular hydrogen bonds usually involve a hydrogen atom that is normally bound to an electronegative atom such as N, O and interacts by electrostatic forces to another electronegative atom and this kind of weak interactions can enhance the packing arrangement and stability of crystal. It is also responsible for large modifications of the nonlinear polarizabilities [14].

### 3.4 UV-Vis-NIR transmittance studies

The recorded transmittance spectrum of DIDPMH is shown in Figure 10 and it is evident from spectrum that the sample possesses a wide optical transparency in the entire near IR region and a part of the visible region and the attained percentage of transmission were around 99. The lower cut-off wavelength of the DIDPMH crystal was around 489 nm. These data attest the suitability of the title crystal for various optical applications in general and NLO applications in particular.

### 3.5 Fluorescence studies

Fluorescence may be expected generally in molecules that are aromatic or contain multiple conjugated system double bonds with a high degree of resonance stability [15]. The fluorescence emission spectrum was measured in the range 500 to 900 nm and is depicted in Figure 11. Three peaks observed in the spectrum at 535, 554 and 608 nm are indicative of the green-orange fluorescence emission by the title crystal.

### 3.6 Powder SHG measurement

The SHG property of DIDPMH crystals was examined through the modified Kurtz-Perry powder technique [16]. The grown single crystal of DIDPMH was powdered into uniform particle size and packed in a micro capillary of uniform bore. A Q-switched Nd:YAG laser beam of wavelength 1064 nm with an input power of 5.7 mJ/pulse width of 8 ns with a repetition rate of 10 Hz was made to fall on the sample. The output from the sample was monochromated to collect the intensity of 532 nm component. The second harmonic generation is confirmed by the emission of green radiation from the sample. Even though the material belongs to centrosymmetric, it exhibits SHG activity due to intermolecular hydrogen bonding and charge transfer interactions between the donor and acceptor systems. The SHG efficiency of DIDPMH crystal was found to be 0.2 times that of potassium dihydrogen orthophosphate (KDP) crystal and is compared with other reported SHG efficiencies of centrosymmetric materials (Table 6).

### 3.7 Thermal analyses.

The TG-DTA thermogram is depicted in Figure 12. From the TG curve it is inferred that the sample of the title crystal undergoes decomposition in a single stage on heating above 275°C. During the decomposition process the material is converted into volatile gaseous products like NO<sub>2</sub>, NO, NH<sub>3</sub> etc. The residue that remains at 497.9°C may be the aromatic hydrocarbons (46.43 %). The DTA curve indicates the same changes shown by TG curve. The DTA trace shows an endothermic peak at about 86.7°C which is due to the dehydration of the DIDPMH complex. The endothermic peak in DTA at 212.9°C corresponds to the melting point of the crystal sample. Another peak at 298.5°C is attributed to the major decomposition temperature. The same results are obtained from DSC.

The DSC trace (Figure 13) of DIDPMH indicates that the endothermic peak at 90.4°C is due to the dehydration of the title crystal. It is clearly seen that there is an endothermic peak starting at 212.8°C corresponds to the melting point of the substance. The exothermic dip at 298.9°C corresponds to the decomposition of the DIDPMH complex into various gaseous products.

### 3.8 Scanning electron microscopy

The SEM micrograph of the title crystal is shown in Figure 14. It is seen from the figure that the DIDPMH complex exhibits the cylindrical shape-like structure with an average particle size of 15-35 μm. This may be due to solvent inclusions, which is generally observed in solution grown crystals.

## 4. CONCLUSION

The single crystals of Diimidazolium dipicrate monohydrate were grown by slow evaporation solution growth technique using dry acetonitrile as the solvent at ambient temperature. FT-IR and NMR spectroscopic studies confirm the formation of DIDPMH complex. Single crystal X-ray diffraction analysis shows that the title crystal belongs to monoclinic crystal system with space group P2<sub>1</sub>/m. UV-Vis-NIR transmission study confirms that the title crystal is suitable for various optical applications. The fluorescence emission study confirms a green-orange emission from the title crystal. The SHG activity in the complex crystal was confirmed by employing Nd:YAG laser as source for IR radiation of wavelength 1064 nm. The SEM micrograph of DIDPMH indicates that the crystal exhibits the cylindrical shape like structure with an average particle size of 15-35 μm. Both TG-DTA and DSC analysis techniques jointly confirm the melting point and decomposition temperature of the crystal.

Wave number (cm <sup>-1</sup> )	Assignment of vibration
3339	OH asymmetric stretching vibration
3147	N <sup>+</sup> -H stretching vibration
3083	Aromatic C-H asymmetric stretching /C-H asymmetric stretching vibration of imidazolium ring
2920	Aromatic C-H symmetric stretching
2998	C-H symmetric stretching vibration of imidazolium ring
1607, 1486	Aromatic C=C stretching
1550	NO <sub>2</sub> asymmetric stretching
1323	NO <sub>2</sub> symmetric stretching
1280	O-H inplane bending
1166	C-O stretching
1089	C-H inplane bending

**Table 1 FT IR spectral band assignments of DIDPMH**

Empirical formula	$C_9H_8N_5O_{7.50}$
Formula weight	306.20
Temperature	293(2)K
Wavelength	0.71073 Å
Crystal system, space group	Monoclinic, $P2_1/m$
Unit cell dimensions	$a=6.8527(3)\text{Å}$ , $\alpha=90^\circ$ $b=23.4396(2)\text{Å}$ , $\beta=111.8120(10)^\circ$ $c=8.1335(6)\text{Å}$ , $\gamma=90^\circ$
Volume	$1212.91(10)\text{Å}^3$
Z, Calculated density	4, 1.677 mg/m <sup>3</sup>
Absorption coefficient	0.148 mm <sup>-1</sup>
F(000)	628
Crystal size	0.30×0.20×0.01 mm
Theta range for data collection	2.70 to 25.00°
Limiting indices	$-8 \leq h \leq 8$ , $-27 \leq k \leq 27$ , $-9 \leq l \leq 9$
Reflections collected/unique	19489/2188 [R(int)=0.0830]
Completeness to theta = 25.00	100.0 %
Absorption correction	Semi-empirical from equivalents
Max. and min. transmission	0.9965 and 0.9235
Refinement method	Full-matrix least-squares on $F^2$
Data/restraints/parameters	2188/1/216
Goodness-of-fit on $F^2$	1.217
Final R indices [ $I > 2\sigma(I)$ ]	R1=0.0797, wR2=0.1624
R indices (all data)	R1=0.0872, wR2=0.1659
Largest diff. peak and hole	0.335 and -0.356 e.Å <sup>-3</sup>

**Table 2 Crystallographic data for DIDPMH**

---

C(1) –C(6)	1.359(6)
C(1) –C(2)	1.443(6)
C(1) –N(1)	1.450(6)
C(2) –O(7)	1.247(5)
C(2) –C(3)	1.442(6)
C(3) –C(4)	1.368(6)
C(3) –N(2)	1.459(6)
C(4) –C(5)	1.377(5)
C(5) –C(6)	1.381(5)
C(5) –N(3)	1.428(5)
C(7) –C(7)#1	1.291(9)
C(7) –N(4)	1.303(6)
C(8) –N(4)	1.349(7)
C(10) –C(9)	1.14(3)
C(10) –N(5)	1.323(5)
C(10) –N(6)	1.465(18)
N(1) –O(2)	1.209(6)
N(1) –O(1)	1.219(6)
N(2) –O(3)	1.20(3)
N(2) –O(4)	1.221(6)
N(3) –O(6)	1.219(5)
N(3) –O(5)	1.228(5)
N(5) –C(10)#1	1.323(5)
O(8) –H(8A)	0.849(10)

---

**Table 3 Selected bond lengths in DIDPMH (Å)**

---

C(6) –C(1) €(2)	125.0(4)
C(6) –C(1) N(1)	117.0(4)
O(7) –C(2) €(3)	124.2(4)
C(3) –C(2) €(1)	111.1(4)
C(4) –C(3) €(2)	124.8(4)
C(4) –C(3) N(2)	115.8(4)
C(3) –C(4) €(5)	119.2(4)
C(4) –C(5) €(6)	120.7(4)
C(4) –C(5) N(3)	119.4(4)
C(6) –C(5) N(3)	119.9(4)
C(1) –C(6) €(5)	119.3(4)
C(7)#1 –C(7) N(4)	108.8(3)
C(7)#1 –C(7) H(7)	125.6
N(4) –C(8) H(8)	127.8
N(4)#1 –C(8) H(8)	127.8
C(9) –C(10) N(5)	114(2)
C(9) –C(10) N(6)	10(3)
N(5) –C(10) N(6)	104.8(14)
O(2) –N(1) Ø(1)	123.4(5)
O(2) –N(1) €(1)	119.6(5)
O(1) –N(1) €(1)	117.0(5)
O(3) –N(2) Ø(4)	113.2(13)
O(3) –N(2) €(3)	126.8(16)
O(4) –N(2) €(3)	118.1(4)
O(6) –N(3) Ø(5)	122.1(4)
O(6) –N(3) €(5)	118.8(4)
O(5) –N(3) €(5)	119.1(3)
C(7) –N(4) €(8)	109.0(5)
C(10) –N(5) €(10)#1	109.9(6)
C(10) –N(5) H(5)	125.0
C(10)#1 –N(5) H(5)	125.0



C(10) -C(9) C(9)#1	101(2)
C(10) -C(9) H(9)	129.6
C(9)#1 -C(9) H(9)	129.6

Table 4 Selected bond angles in DIDPMH (°)

D-H...A	d(D-H)	d(H...A)	d(D...A)	<(DHA)
N(4) -H(4A)...O(6)#2	0.86	2.34	3.066(6)	142.8
N(4) -H(4A)...O(1)#3	0.86	2.57	3.185(6)	129.5
N(5) -H(5)...O(8)	0.86	1.85	2.701(7)	170.5
O(8) -H(8A)...O(7)#4	0.849(10)	1.97(2)	2.790(4)	162(6)
N(6) -H(9')...O(7)#5	0.86	2.22	3.03(3)	157.0

#1 x, -y+1/2, z; #2 -x+2, -y, -z+1; #3 x, y, z-1; #4 x, -y+1/2, z-1; #5 x+1, y, z.

Table 5 Hydrogen bond parameters in DIDPMH

Sample	Space group	SHG efficiency in comparison with KDP
(p-Nitrophenol, hexa methylaminetetramine, phosphoric acid and water) supermolecular crystal [17]	P2 <sub>1</sub> /c	3.1
R, S - serine [18]	P2 <sub>1</sub> /a	0.02
Glycine picrate [19]	P2 <sub>1</sub> /a	2.34
Heptaqua-4-nitrophenolato strontium (I) nitro phenol [20]	pbca	0.42
Guanidium Trifluoroacetate [21]	pbcn	0.87
Diimidazolium dipicrate monohydrate [present work]	P2 <sub>1</sub> /m	0.2

Table 6 SHG efficiencies of centrosymmetric crystals compared with KDP

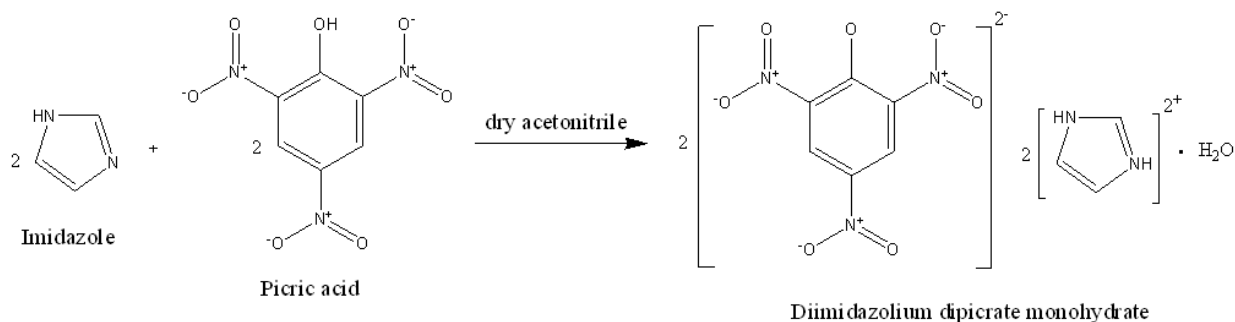


Figure 1 Reaction scheme of DIDPMH



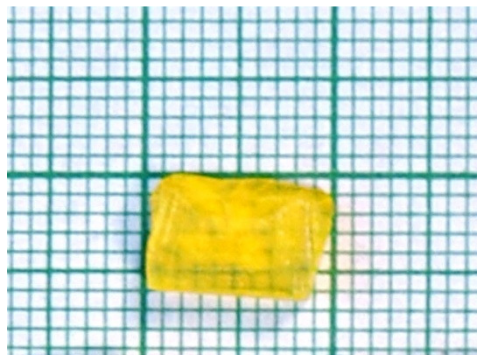


Figure 2 As-grown single crystal of DIDPMH

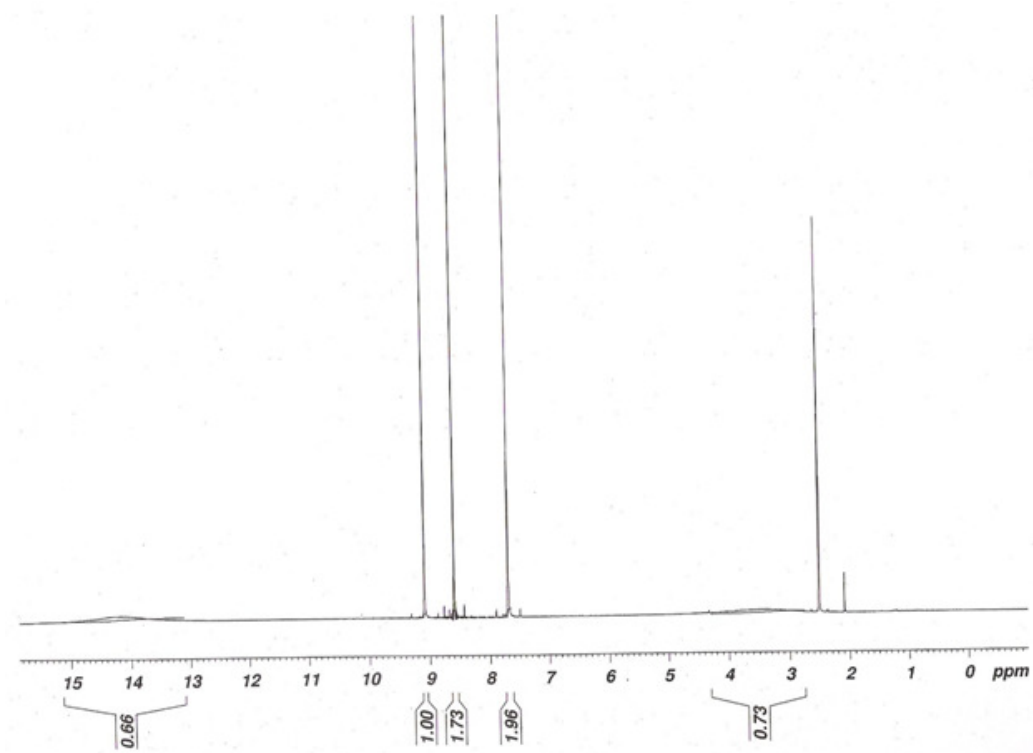
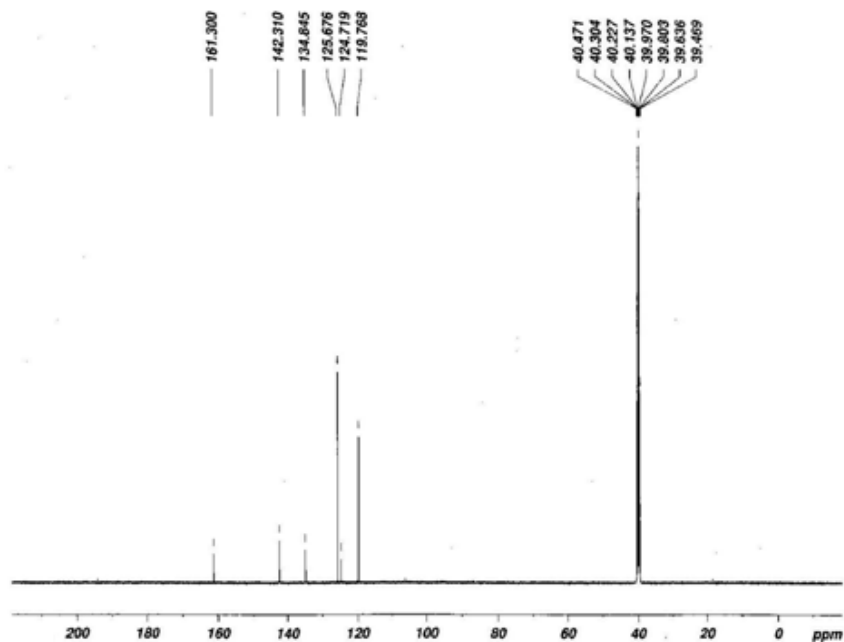
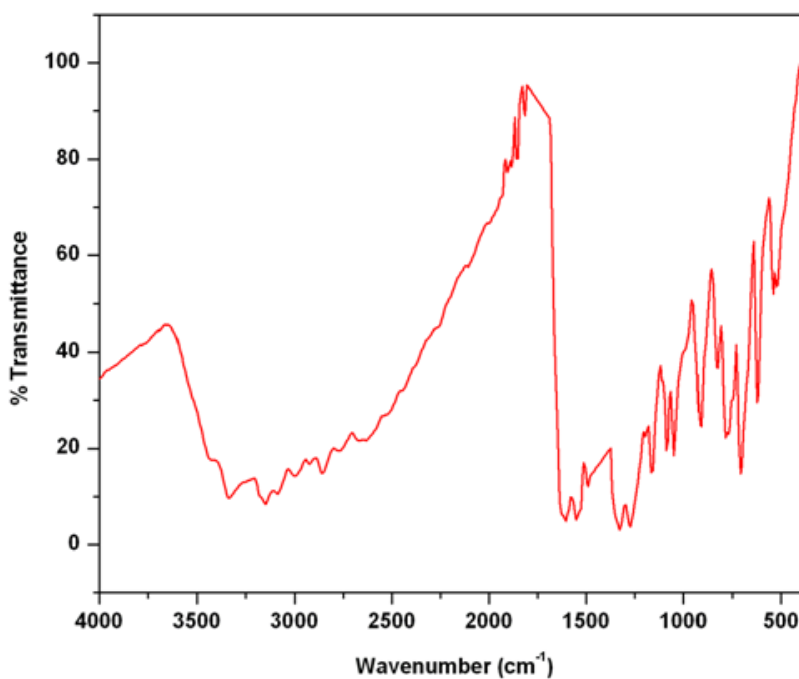


Figure 3  $^1\text{H}$  NMR Spectrum of DIDPMH



**Figure 4**  $^{13}\text{C}$  NMR Spectrum of DIDPMH



**Figure 5** FT IR Spectrum of DIDPMH

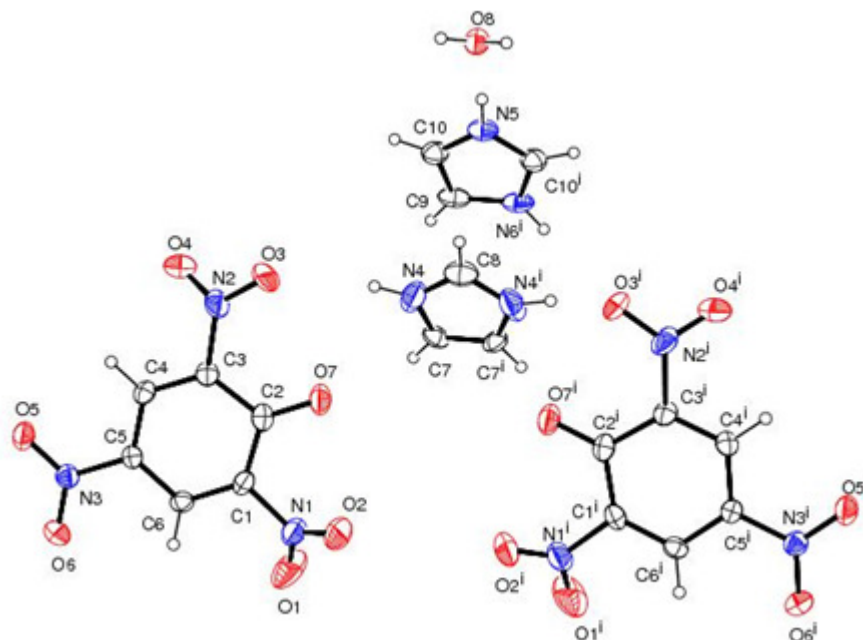


**Figure 6** ORTEP plot of DIDPMH

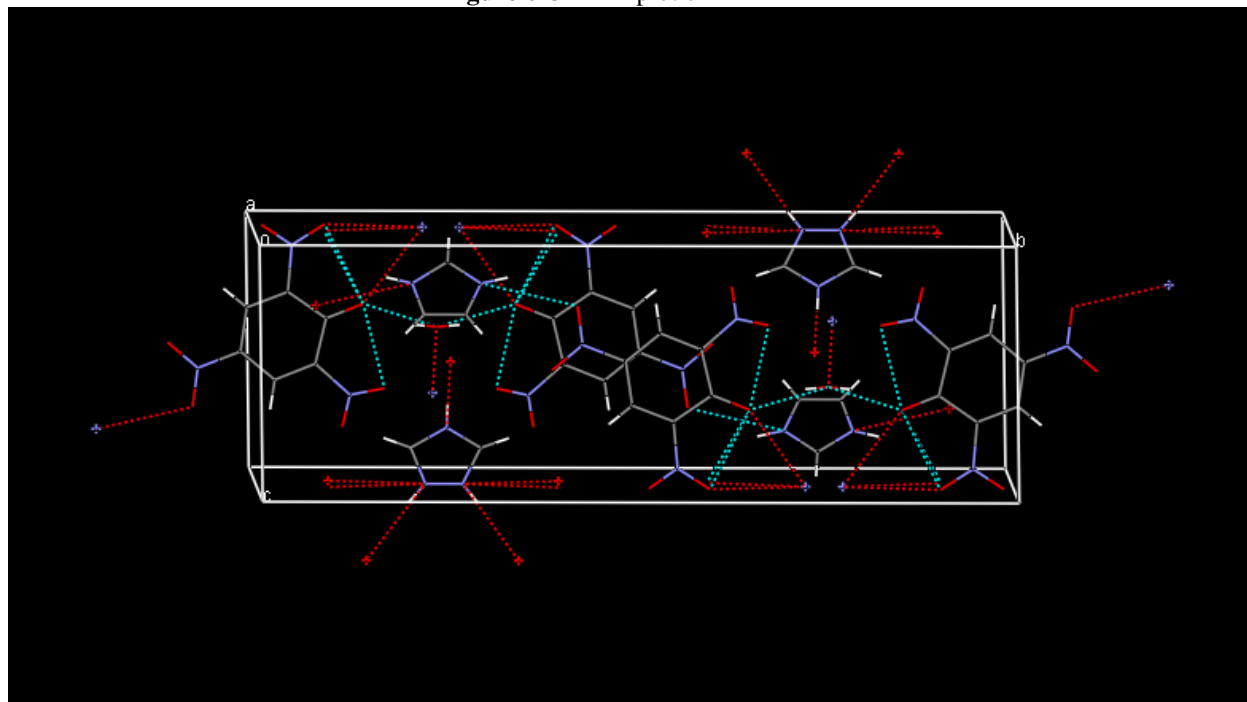


**Figure 7** Molecular packing arrangement of DIDPMH viewed down 'c' axis.

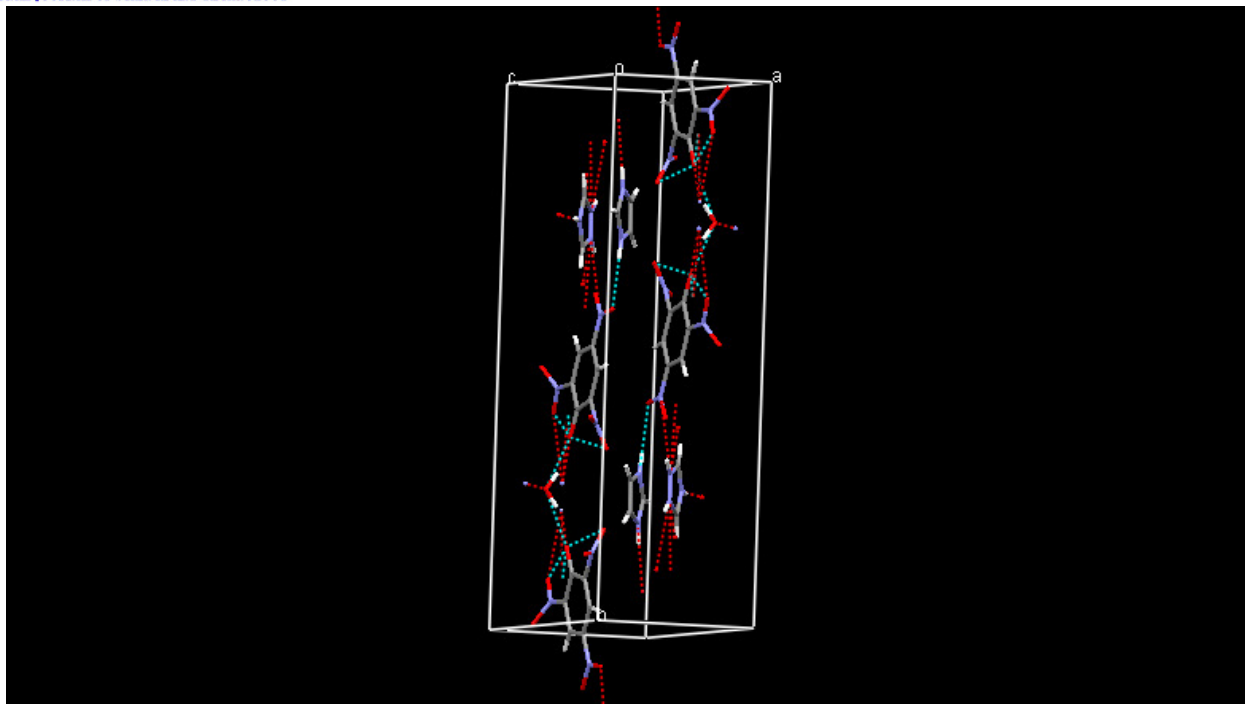


**Figure 8** Molecular packing arrangement of DIDPMH viewed down 'b' axis.

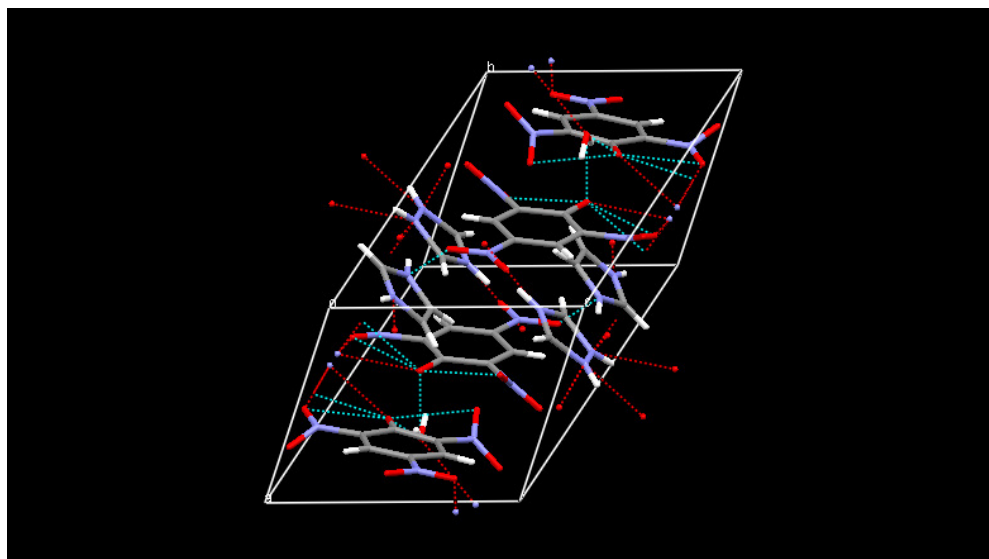


**Figure 9** Molecular packing of DIDPMH showing intermolecular N-H...O and O-H...O hydrogen bonds in three dimensional network.

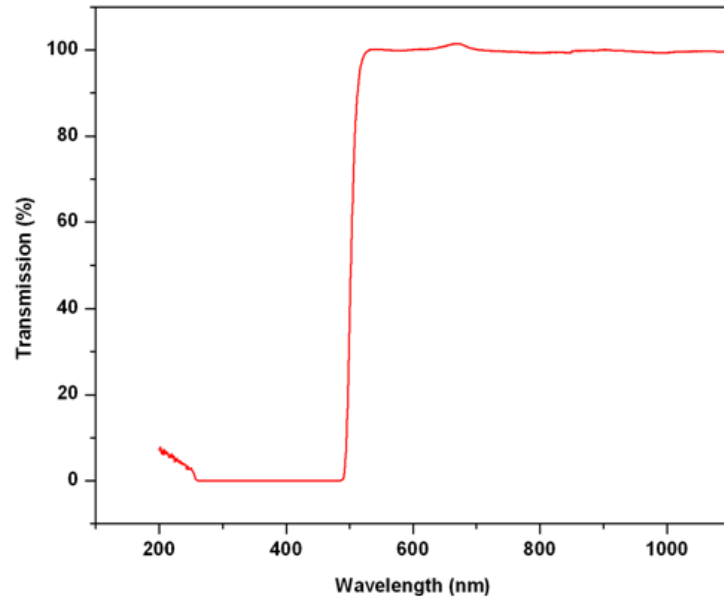


**Figure 10** Optical transmission spectrum of DIDPMH

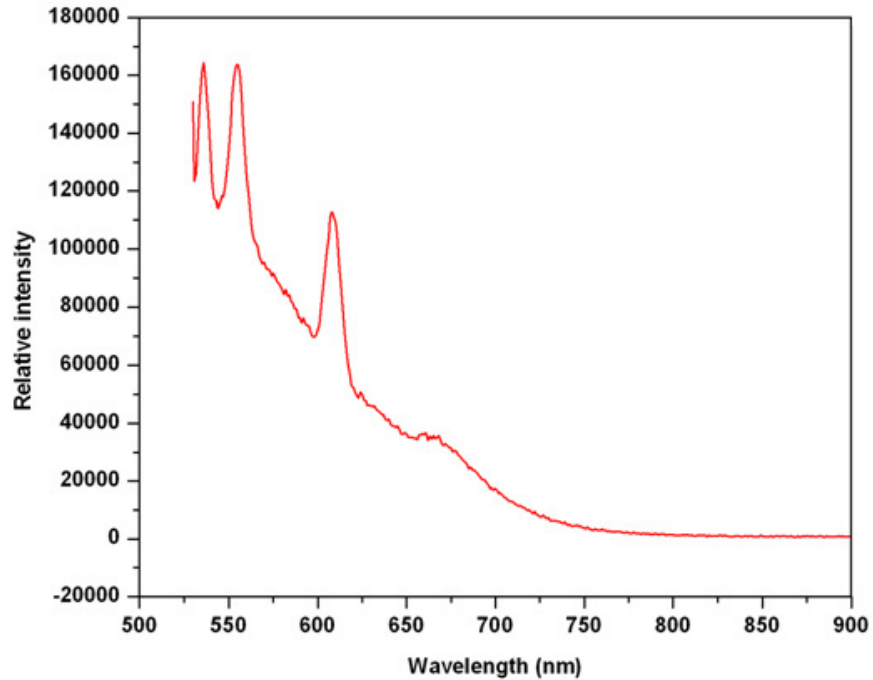


**Figure 11.** Fluorescence emission spectrum of DIDPMH

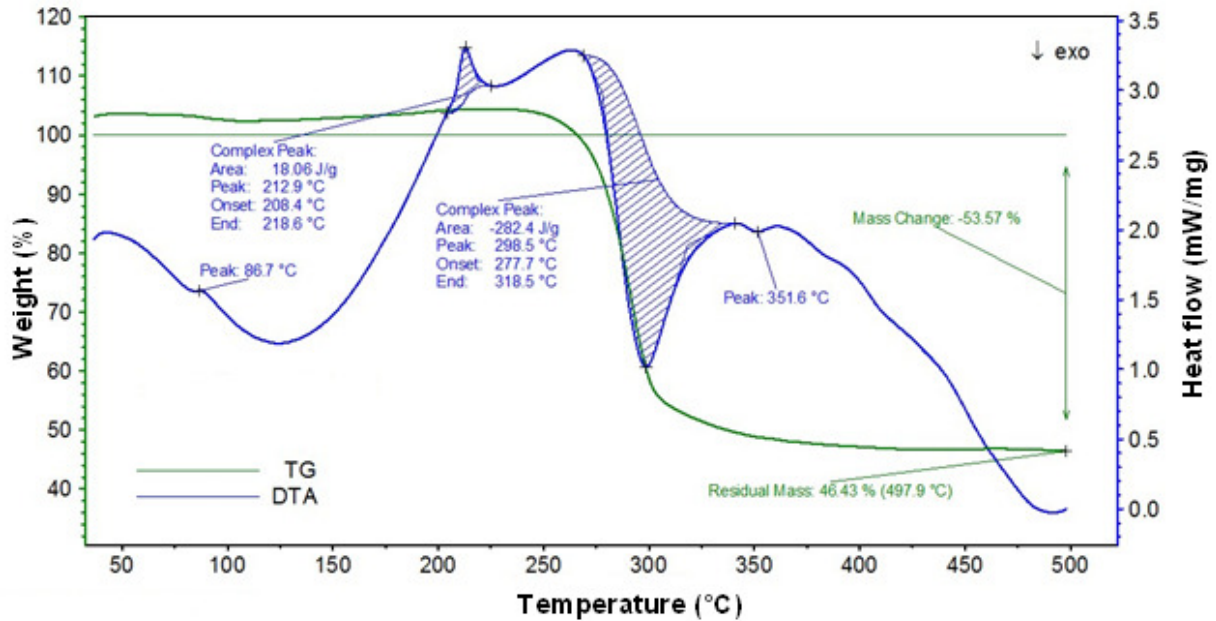


Figure 12 TG/DTA spectra of DIDPMH

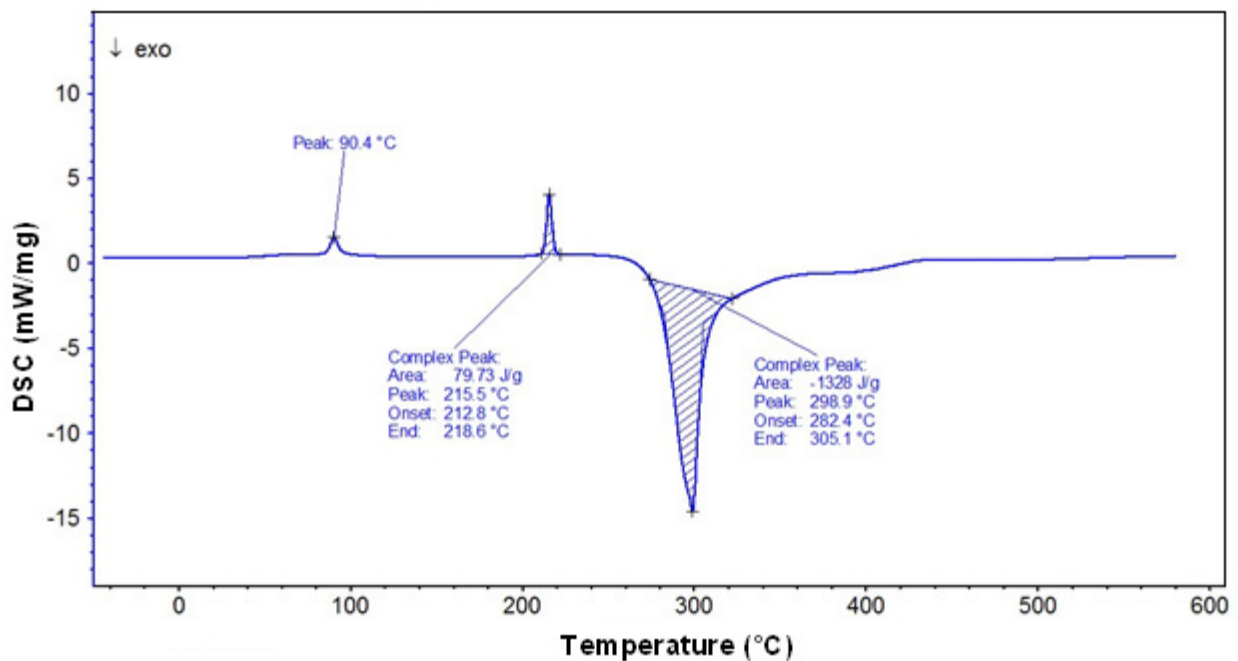
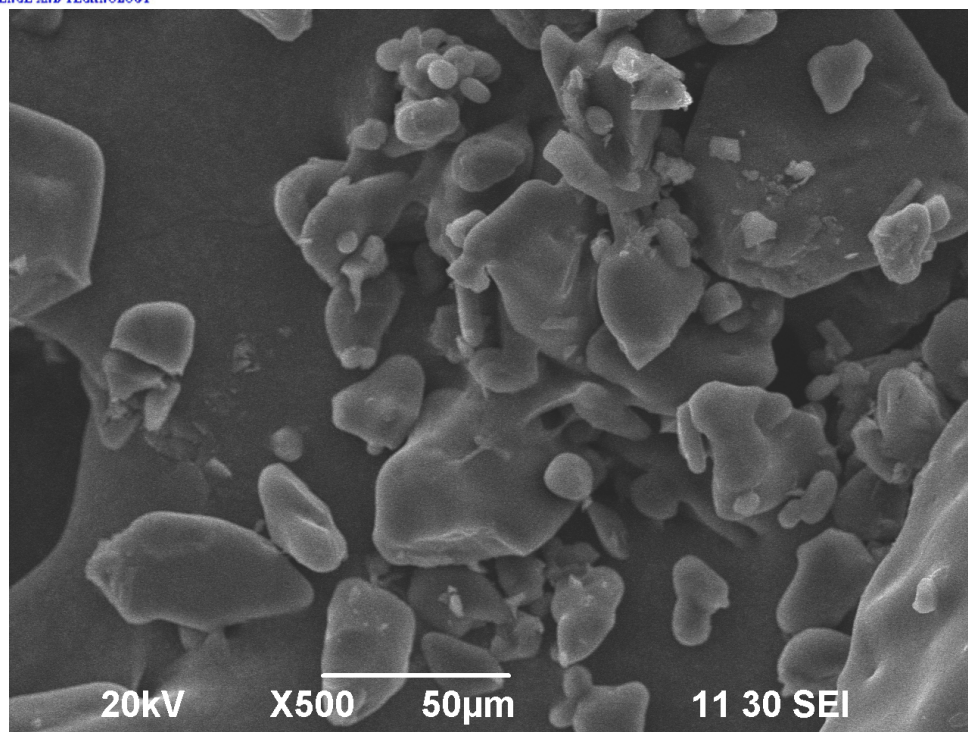


Figure 13 DSC Spectrum of DIDPMH



**Figure 14** SEM image of as grown DIDPMH

### Supplementary information

The crystallographic information file has been deposited by us in the Cambridge structure database (CCDC 884222). These data can be obtained by free of charge from The Cambridge Crystallographic Data Center via [www.ccdc.cam.ac.uk/data-request/cif](http://www.ccdc.cam.ac.uk/data-request/cif).

### REFERENCES

1. Tatiana Caneque, Ana M. Cuadro, Julio Alvarez-Builla, Juan J. Vaquero, *Tetrahedron Lett.*, 50, 1419 (2009).
2. L. R. Dalton, *Pure Appl. Chem.*, 76, 1421 (2004).
3. P. N. Prasad, D. J. Williams, *Introduction to Nonlinear Optical Effects in Molecules and Polymers*, Wiley, New York, 1991.
4. S. Gowri, T. Uma Devi, D. Sajan, S. R. Bheeter, N. Lawrence, *Spectrochim. Acta A*, 89, 119 (2012).
5. C. Sridevi, G. Velraj, *J. Mol. Struct.*, 1019, 50 (2012).
6. A. R. Katritzky, C. W. Rees, *Comprehensive Heterocyclic Chemistry*, oxford: pergamon 5, 469 (1984).
7. Jayaraman Jayabharathi, Venugopal Thanikachalam, Natesan Srinivasan, Karunamoorthy Jayamoorthy, *Spectrochim. Acta A*, 83, 329 (2011).
8. Jayaraman Jayabharathi, Marimuthu Venkatesh Perumal, Venugopal Thanikachalam, *Spectrochim. Acta A*, 95, 497 (2012).
9. M. Soriano-Garcia, M. Schatz-Levine, R. A. Toscano, R. Villena Iribe, 1990 *Acta Cryst.*, C46 1556 (1990).
10. Herbstein, Moshe Kapon, *Acta Cryst.*, C47, 1131 (1991).
11. S. Anandhi, T. S. Shyju, T. P. Srinivasan, R. Gopalakrishnan, *J. Cryst. Growth*, 335 75 (2011).
12. Rodolfo Moreno-Fuquen, Regina De Almeida Santos, Lina Aguirre, *Acta Cryst.*, E67, O139 (2011).



INTERNATIONAL JOURNAL OF SCIENCE AND TECHNOLOGY

13. G. M. Sheldrick, SHELXL-97, Program for X-ray Crystal Structure Refinement, University of Gottingen, Germany, 1997.
14. G. Venkatesan, G. Anandha Babu, P. Ramasamy, A. Chandramohan, Vivek K. Gupta, Rajnikant, Solid state sci., 14, 1141 (2012).
15. H. H. Willard, L. L. Merritt, J. A. Dear, F. A. Settle, Instrumental Methods of Analysis, Sixth ed., Wadsworth Publishing Company, USA, 609 (1986).
16. S. K. Kurtz, T. T. Perry, J. Appl. Phys., 39, 3798 (1968).
17. Guo Wensheng, Guo Fang, Wei Chun Sheng, Liu qitao, Zhou Guangyong, Wang Dong, Shao Zhongshu, Sci. China, Ser B: chem., 45, 267 (2002).
18. K. E. Rieckhoff, W. L. Peticolas, Science, 147, 610 (1965).
19. Mohd. Shakir, S. K. Kushwaha, K. K. Maurya, Manju Arora, G. Bhagavannarayana, J. Cryst. Growth, 311, 3871 (2009).
20. M. Jose, B. Sridhar, G. Bhagavannarayana, K. Sugandhi, R. Uthrakumar, C. Justin Raj, D.Tamil Vendhan, S. Jerome Das, J. Cryst. Growth, 312, 793 (2010).
21. M. Loganayaki, V. Siva Shankar, P. Ramesh, M. N. Ponnuswamy, P. Murugakoothan, The Journal of Minerals and Materials Characterization and Engineering, 10, 843 (2011).

**K. MOHANA PRIYADARSHINI, A. CHANDRAMOHAN\***

Department of Chemistry, Sri Ramakrishna Mission Vidyalaya College of Arts and Science,  
Coimbatore, Tamilnadu, India.